

Article

Optimizing Ex Vivo CAR-T Cell-Mediated Cytotoxicity Assay through Multimodality Imaging

John G. Foulke, Luping Chen, Hyeyoun Chang , Catherine E. McManus , Fang Tian * and Zhizhan Gu * 

American Type Culture Collection (ATCC), Manassas, VA 20110, USA

* Correspondence: ftian@atcc.org (F.T.); zgu@atcc.org (Z.G.)

Simple Summary: CAR-T cell therapies are highly effective for treating cancers, particularly liquid tumors, and are now being tested in clinical trials for solid tumors. The FDA's initiative for new drug discovery methods highlights the need for precise ex vivo assays for CAR-T development. Current assays have drawbacks, such as using radioactive materials and lacking real-time measurement and automation. To improve these assays, we used multimodality imaging (bioluminescence, impedance, phase contrast, and fluorescence) to monitor CAR-T cells with cancer cells in real-time. We also adjusted cell ratios for optimal results. Our optimized assay showed that CAR-T cells effectively attacked cancer cells, providing precise, reliable, and high-throughput measurements.

Abstract: CAR-T cell-based therapies have demonstrated remarkable efficacy in treating malignant cancers, especially liquid tumors, and are increasingly being evaluated in clinical trials for solid tumors. With the FDA's initiative to advance alternative methods for drug discovery and development, full human ex vivo assays are increasingly essential for precision CAR-T development. However, prevailing ex vivo CAR-T cell-mediated cytotoxicity assays are limited by their use of radioactive materials, lack of real-time measurement, low throughput, and inability to automate, among others. To address these limitations, we optimized the assay using multimodality imaging methods, including bioluminescence, impedance tracking, phase contrast, and fluorescence, to track CAR-T cells co-cultured with CD19, CD20, and HER2 luciferase reporter cancer cells in real-time. Additionally, we varied the ratio of CAR-T cells to cancer cells to determine optimal cytotoxicity readouts. Our findings demonstrated that the CAR-T cell group effectively attacked cancer cells, and the optimized assay provided superior temporal and spatial precision measurements of ex vivo CAR-T killing of cancer cells, confirming the reliability, consistency, and high throughput of the optimized assay.

Keywords: CAR-T; cytotoxicity assay; multimodality imaging; CD19; CD20; HER2



Citation: Foulke, J.G.; Chen, L.; Chang, H.; McManus, C.E.; Tian, F.; Gu, Z. Optimizing Ex Vivo CAR-T Cell-Mediated Cytotoxicity Assay through Multimodality Imaging. *Cancers* **2024**, *16*, 2497. <https://doi.org/10.3390/cancers16142497>

Academic Editor: Shebli Atrash

Received: 11 June 2024

Revised: 2 July 2024

Accepted: 6 July 2024

Published: 9 July 2024



Copyright: © 2024 by the authors. Licensee MDPI, Basel, Switzerland. This article is an open access article distributed under the terms and conditions of the Creative Commons Attribution (CC BY) license (<https://creativecommons.org/licenses/by/4.0/>).

1. Introduction

CAR-T therapy, also known as chimeric antigen receptor T-cell therapy, is an innovative and promising form of immunotherapy that has revolutionized the field of cancer treatment [1]. This cutting-edge therapy involves reprogramming a patient's own T cells to express a chimeric antigen receptor (CAR) specific to tumor-associated antigens (TAAs) [2]. By genetically modifying T cells to recognize and target cancer cells with precision, CAR-T therapy offers a personalized and targeted approach to treat various types of hematological malignancies and solid tumors. The remarkable success of CAR-T therapy in clinical trials and its approval for certain indications, such as leukemias, lymphomas, and multiple myelomas, has marked a significant breakthrough in cancer treatment [3–6]. As ongoing research continues to refine CAR-T cell design, improve safety profiles, and expand the range of treatable cancers, this transformative therapy holds the potential to reshape the landscape of oncology and pave the way for more effective and personalized cancer therapies.

Considerable research efforts have been invested into developing new CAR structures to increase the scope of targeted cancer types and raise their anti-tumor efficacy [7]. One of the bottlenecks in the process of CAR-T development is evaluating the biofunction of CAR-T cells *ex vivo*. Despite the growing importance of *ex vivo* CAR-T cell cytotoxicity assays as a valuable means of assessing CAR-T cell functionality and effectiveness, there are still various challenges and limitations that need to be addressed. These include a simplified tumor microenvironment, limited immune system interactions, artificial activation and expansion, lack of dynamic monitoring, inadequate assessment of CAR-T cell exhaustion, and variability in assay techniques [8].

As recently reviewed in *Nature Protocols*, the prevailing *ex vivo* CAR-T cytotoxicity assays are the chromium (^{51}Cr)–release assay (^{51}Cr assay), the luciferase-mediated bioluminescence imaging (BLI) assay, the impedance-based assay, and the flow cytometry assay (flow assay) [8]. However, each of these assays has its own limitations. For example, the chromium–release assay is a commonly used method to measure target cell lysis by CAR-T cells. It involves labeling target cells with a radioactive chromium isotope, which is released into the supernatant upon target cell lysis [9]. While widely used, the limitations of this assay include radioactivity, lack of dynamic monitoring, non-specific release, insensitivity to low levels of killing, and delayed measurements [10–12]. The flow cytometry assay is a widely used technique for evaluating CAR-T cell cytotoxicity by measuring target cell death or marker expression. However, it also has some limitations, such as limited dynamic range, lack of spatial information, influence of non-specific binding, and limitations of fluorophores. The impedance-based assay is limited by its lack of specificity, insufficient sensitivity, difficulty in multiplexing, indirect measurement, and insensitivity to low-level cytotoxicity, etc. The limitations of the bioluminescence imaging assay commonly include signal attenuation, lack of spatial information, signal persistence, background noise, and limited resolution [8,12,13].

Overall, every single *ex vivo* CAR-T cell-mediated cytotoxicity assay has various limitations due to the assay technology itself. We generated a panel of luciferase reporter tumor cell lines that can be used to examine the function of CAR-T cells. The reporter cells in this panel naturally express high levels of clinically relevant CAR-T target antigens on the cell surface, such as CD19, CD20, and HER2. By utilizing stable luciferase expression in these CAR-T target tumor cell lines, we can enhance the *ex vivo* CAR-T cell-mediated cytotoxicity assay by employing multimodality imaging techniques. This approach allows us to overcome certain limitations associated with individual single assay methods, such as radioactivity and the absence of spatial information, while optimizing overall assay performance.

2. Materials and Methods

2.1. Cell Culture, Lentiviral Transfection, and Single Cell Cloning

The following cell lines were obtained from ATCC based upon their high expression levels of common CAR-T target antigens and grown according to the ATCC product sheet recommendations: WIL2-S (CD19), Raji (CD19), Daudi (CD20), Farage (CD20), and BT-474 (HER2). Five hundred thousand cells per line were transduced with a lentiviral plasmid expressing luciferase under the control of an EF1A promoter using 50 $\mu\text{g}/\text{mL}$ of protamine sulfate. After viral transduction, Luc2 cell lines were selected and maintained in the same culture media as the parental cell lines but with 4.0–8.0 $\mu\text{g}/\text{mL}$ blasticidin (Gibco, Waltham, MA, USA). After selection, luciferase pools were screened for luciferase activity. Single cells were sorted into 96-well plates using a Sony SH800 automated cell sorter (Sony Biotechnology, San Jose, CA, USA) and expanded for approximately 10–14 days until confluency reached 70%. The single clones were then subcultured and evaluated for luciferase activity again. The single clones that yielded the highest luciferase activity were chosen for further evaluation to verify that the introduction of luciferase into the cell line did not cause changes in growth rate, morphology, and expression of target antigens.

2.2. Co-Culture Setup for CAR-T Cytotoxicity Assays

CAR-T cytotoxicity was studied using CD19 CAR-T, CD20 CAR-T, or HER2 CAR-T cells (ProMab, Richmond, CA, USA), which were each paired with mock CAR-T cells generated from the same donor as a control. CAR-T target luciferase reporter cell lines were seeded at 5×10^3 cells per well into 96-well plates (Corning, Corning, NY, USA) in triplicate in 50 μ L of complete media (without blasticidin). An amount of 50 μ L of CAR-T cells was added to each well to correspond to an effector-to-target ratio (CAR-T cells: Target cells) of 1:1, 2:1, 5:1, or 10:1. The CAR-T target luciferase reporter cells were either pre-stained with Vybrant™ DiO (Thermo Fisher, Waltham, MA, USA), co-cultured in the presence of Incucyte® Cytotox red dye (Sartorius, Göttingen, Germany), or left unstained for the luciferase assay.

2.3. Next Generation Sequencing and Expression Heat Map Generation

RNA sequencing was performed in duplicate for Raji and WIL2-S cell lines and their paired Luc2 daughter lines. Library preparation using the TruSeq Stranded mRNA library prep kit (Illumina, San Diego, CA, USA) and 150 bp paired-end sequencing on a NovaSeq6000 S4 were performed at Psomagen (Rockville, MD, USA). Then, the reads were aligned to hg38 using HISAT2 (v2.1.0), and transcripts were assembled using StringTie (v2.1.3b) at Psomagen. Expression heat maps were generated using Microsoft Excel software version 2308 for 12 hematologic tumor CAR-T targets and 26 solid tumor CAR-T targets either using the Cancer Cell Line Encyclopedia (CCLE) database (Broad Institute, Cambridge, MA, USA) or the in-house bulk RNA-seq results. The CCLE values are $\log_2(\text{TPM} + 1)$ according to the CCLE public data guidance. The in-house RNA-seq values are $\log_2(\text{FPKM} + 1)$. A brief summary of the in-house RNAseq results is as follows: Whole transcriptome sequencing was performed in order to examine the gene expression profiles and perform gene annotation on a set of useful genes based on gene ontology pathway information. Analyses were successfully performed on all paired-ends samples. Trimmed reads were mapped to reference genome with HISAT2. After the read mapping, StringTie was used for transcript assembly. The expression profile was calculated for each sample and transcript/gene as read count and FPKM (Fragment per Kilobase of transcript per Million mapped reads).

2.4. Luminescence Assay

CAR-T cytotoxicity co-culture was performed as previously described. After 24 h of co-culturing, an equal volume of Bright-Glo™ Reagent (Promega, Madison, WI, USA) was added to the cells. After 8 min of incubation at room temperature on a plate shaker, reactions were transferred to a white opaque plate, and luminescence was measured on a SpectraMax i3x plate reader (Molecular Devices, San Jose, CA, USA). Luminescence was normalized to wells with no CAR-T cells and was plotted as fold change in Prism 9 v9.0.0 (121) (Graphpad, San Diego, CA, USA).

2.5. Real-Time xCELLigence Live Cell Analysis

BT-474-Luc2 cells (2×10^4 cells/well) were seeded in 96-well RTCA E-Plate (Agilent, Santa Clara, CA, USA) and left to adhere for 24 h. On the day of the co-culture cytotoxicity experiments, HER2 CAR-T cells or mock CAR-T cells from the same donor were added at an effector/target cell ratio of 10:1 and measured in a real-time cell analysis assay using the xCELLigence SP system (Agilent, Santa Clara, CA, USA). An electrical current was applied to each co-culture. E-plates were read every 15 min for 24 h, and data were normalized to starting resistance. The normalized cell index was plotted as fold change against time in Prism 9 v9.0.0 (121) (Graphpad, San Diego, CA, USA).

2.6. DiO Staining for Live Cell Imaging

An amount of 5 μ L of Vybrant DiO cell labeling solution (Molecular Probes, Eugene, OR, USA) was added to 1 mL of serum-free RPMI-1640 media (ATCC, Manassas, VA, USA),

premixed by vortexing, and used to resuspend Raji-Luc2 cells at 1×10^6 cells/mL. Cells were transferred to a 12-well plate and incubated at 37 °C for 45 min with agitation every 5–10 min. Cells were pelleted by centrifugation and washed 3× with fresh culture media. Cells were plated and allowed to recover overnight prior to seeding into a 96-well plate for co-culture experiments. After the co-culture assay was set up, green fluorescent and brightfield images were captured with the Cytation1 plate reader (Agilent, Santa Clara, CA, USA) using a 4× objective to capture 2 × 2 image montages in 30 min intervals for 24 h. Images were stitched using Gen 5 v3.11 software (Agilent, Santa Clara, CA, USA).

2.7. Cytotox Red Dye Staining for Live Cell Imaging

CAR-T cytotoxicity co-culture was set up, as previously mentioned, into 96 well plates. Cytotox Red (Sartorius, Göttingen, Germany) was diluted to a stock of 100 uM using DPBS and then was used at a final concentration of 250 nM in the well. Red fluorescent and brightfield images were captured with the Cytation1 plate reader (Agilent, Santa Clara, CA, USA) using a 4× objective to capture 2 × 2 image montages in 1 h intervals for 24 h. Images were stitched using Gen 5 v3.11 software (Agilent, Santa Clara, CA, USA). Red fluorescent intensity was either measured using Gen5 software or ImageJ v1.53t (NIH, Bethesda, MD, USA).

2.8. NK Direct Killing and ADCC Assay

The 2×10^6 naive NK cells (ATCC, Manassas, VA, USA) were stimulated with MACS beads (Miltenyi Biotec, Bergisch Gladbach, Germany) and cultured for 7 days for expansion. Luciferase-expressing cells were seeded at 5.0×10^3 cells/well in triplicate into 96-well plates using RPMI + 10% low IgG FBS medium. Various ratios of target cells to effector cells ranging from 1:4 to 16:1 were tested for direct cell killing via luminescence. To perform the ADCC assay, a 96-well plate was set up with Rituximab (anti-CD20), Trastuzumab (anti-HER2), or isotype control mAb antibody (Invivogen, San Diego, CA, USA) at concentrations from 10 µg/mL diluting down to 0.0001 µg/mL. The 5×10^3 target cells and 2.5×10^3 NK cells were added for a 2:1 target-to-effector cell ratio. Co-cultures were incubated for 4 h. Then, 100 µL of the co-culture was transferred to a white plate with an equal volume of Bright-Glo reagent (Promega, Madison, WI, USA) and was incubated for 5 min before luminescence was measured.

2.9. Flow Cytometry

For the flow cytometry analyses, cells were stained with the following fluorescently labeled antibodies specific for CAR-T target antigens on the cell surface: APC anti-CD19, FITC anti-CD20, and PE anti-HER2 (Miltenyi Biotec, Bergisch Gladbach, Germany). PE, APC, or FITC-conjugated human IgG1 (Miltenyi Biotec) was used as an isotype control. Cell staining was performed in Fetal Bovine Serum Stain Buffer (BD Biosciences™) with the antibodies diluted to the manufacturer's recommended concentrations for 30 min on ice in the dark. Cells were then fixed by the addition of an equal volume of Fixation Buffer (BD Biosciences™). For each sample, 10,000 stained cells were captured by the Accuri C6 Plus flow cytometer (BD), and the results were analyzed using the FlowJo® software version v10.9.0.

3. Results

3.1. mRNA Profiling of Cancer Cell Lines for Common CAR-T Targets

Over 30 luciferase-expressing cell lines have been generated at ATCC and are maintained in the extensive cancer cell line collection. To identify the best candidate lines for CAR-T cytotoxicity assay development, we examined expression data from the CCLE database for transcript levels of 12 common hematological tumor CAR-T targets and 26 common solid tumor CAR-T targets [14,15]. Data were available for the parental cell lines of 16 existing luciferase-expressing lines at ATCC representing 16 different tissue and cancer types. We created a heatmap in which genes were colored red to indicate high expression and blue to indicate low expression (Figure 1). Few cell lines with existing ATCC luciferase reporters have high levels of CD19 or BCMA, the only two FDA-approved CAR-T

targets as of now [16]. When we examined expression data for additional ATCC parental cancer cell lines without already existing luciferase reporters, we found that the lymphoma cell lines Raji, Farage, and Daudi express high levels of CD19, as well as high levels of CD20, CD22, and CD38. In addition, BT-474, a breast ductal carcinoma cell line, expresses high levels of HER2, another very popular CAR-T target in solid tumors currently under investigation [17]. WIL2-S, a B lymphoblast cell line, did not have available expression data in the CCLE database but was included due to known high levels of CD20 [18]. In-house RNAseq experiments confirmed high expression of CD19, CD20, CD22, and CD70, etc., in both WIL2-S and RAJI cell lines (Figure 2A). Overall, these results show that key CAR-T targets are endogenously expressed at high levels in these cell lines, making them good candidates for generating CAR-T target luciferase reporter lines. In addition, this analysis can be used to determine which luciferase-expressing cell lines available from ATCC could be good candidates for use in studies of other CAR-T targets such as LeY, ROR1, or WT1 in hematological tumors and MET, CD70, or EPCAM in solid tumors [14,15].

We, therefore, generated five new luciferase reporter cell lines for potential use in CAR-T cell therapy research: Raji-Luc2, WIL2-S-Luc2, BT-474-Luc2, Daudi-Luc2, and Farage-Luc2 (Figure 2B). A lentiviral plasmid was transduced into these ATCC-authenticated tumor cell lines, and single-cell cloning was performed to generate a homogenous culture, which was expanded and validated for luciferase expression. Single clones with high luciferase activity were further characterized by comparing their morphology and growth kinetics to their parental cell lines, which revealed high similarity between parental and daughter Luc2 lines (Figures S1 and S2). High expression levels of endogenous CAR-T target antigens in the reporter lines were also verified by flow cytometry (Figure S3). Finally, the reporter lines showed luciferase expression that increased linearly with cell number and was stable over at least 30 generations (Figures S4 and S5).

To compare the expression levels of CAR-T target antigens in engineered versus parental lines, mRNA sequencing was performed on cell pellets isolated from WIL2-S, WIL2-S-Luc2, Raji, and Raji-Luc2 in duplicate. The results confirmed that common CAR-T target expression in the Raji and WIL2-S parental and daughter lines remains unaffected by the introduction of luciferase (Figure 2A).

Cell Line Info		ATCC LUC2 ID	CRL-8885-LUC2	CCL-86-LUC2	HTB-20-LUC2	CRL-2630-LUC2	CCL-213-LUC2	CCL-121-LUC2	CCL-185-LUC2	CCL-225-LUC2	CCL-228-LUC2	CCL-240-LUC2	CCL-247-LUC2	CRL-1435-LUC2	CRL-1469-LUC2	CRL-1555-LUC2	CRL-1619-LUC2	CRL-1739-LUC2	CRL-2003-LUC2	HTB-14-LUC2	HTB-22-LUC2	HTB-43-LUC2	HTB-96-LUC2
Cell Line Name		WIL2-S	RAJI	BT474	FARAGE	DAUDI	HT1080	A549	HCT15	SW480	HU60	HCT116	PC3	PANC1	A431	A375	AGS	TF1	U87MG	MCF7	FADU	U2OS	
Lineage Subtype		N/A	Non Hodgkin Lymphoma	Breast Ductal Carcinoma	Non Hodgkin Lymphoma	Non Hodgkin Lymphoma	Fibrosarcoma	NSCLC	Colorectal Adenocarcinoma	Colorectal Adenocarcinoma	AML	Colorectal Adenocarcinoma	Prostate Adenocarcinoma	Exocrine	Skin Squamous	Melanoma	Gastric Adenocarcinoma	AML	Glioma	Breast Carcinoma	Upper Aerodigestive Squamous	Osteosarcoma	
Haematological Tumor CAR Targets	TNFRSF17 (BCMA)	N/A	3.8807	0.1635	1.3785	4.1094	0.0000	0.0000	0.0426	0.1243	0.2869	0.0704	0.1110	0.2987	0.0000	0.1375	0.0000	0.0000	0.2388	0.0000	0.0000	0.0000	0.2016
	IL3RA (CD123)	N/A	0.0566	0.2141	0.0000	0.3103	0.1890	0.0841	0.0566	0.1890	0.4436	0.0000	0.0000	0.1635	0.0000	0.1635	0.1110	1.9928	0.0566	0.0566	0.0841	0.3785	
	SDC1 (CD138)	N/A	0.3785	6.2052	0.0144	0.3103	7.1797	6.5703	5.7142	4.7719	6.6229	4.9303	7.6454	6.3425	7.7041	4.5027	5.0866	1.0000	5.7230	3.9653	6.3100	6.3583	
	CD19	N/A	7.1104	0.0000	6.5132	6.9925	0.0841	0.0704	0.0000	0.0144	0.1890	0.0286	0.0426	0.0704	0.0000	0.0144	0.0000	1.6182	0.0000	0.0000	0.0976	0.0426	
	MSA11 (CD20)	N/A	8.0865	0.0000	9.0930	8.8855	0.0704	0.0426	0.1763	0.0000	0.0000	0.1375	0.0000	0.0144	0.0000	0.1110	0.0841	0.1763	0.0000	0.0976	0.0566	0.1243	
	CD22	N/A	7.5211	0.2141	8.6641	9.8023	3.4436	0.2388	0.2510	0.9336	0.0286	2.1210	0.2388	1.0000	2.0000	2.9030	0.5059	3.4141	2.5558	1.5607	0.2141	1.6781	
	CD38	N/A	5.8276	0.0286	3.8032	7.4682	0.0841	2.5008	0.0000	0.0144	0.6041	0.0000	0.0426	0.0976	0.6323	0.0000	0.1110	3.1570	0.1890	0.2016	0.2987	0.0704	
	CD5	N/A	0.0144	0.1506	0.0286	0.0976	0.0286	0.0000	0.0144	0.0144	0.0000	0.0144	0.1506	0.0286	0.0426	0.0144	0.0144	0.0144	0.0144	0.0426	0.1763	0.0144	0.0976
	FUT3 (LeY)	N/A	0.0144	0.1506	0.0566	0.0841	0.0000	0.0286	1.7442	0.0426	0.0426	0.1506	2.4222	0.0566	2.8875	0.0841	0.1763	0.0286	0.1110	0.1763	3.7560	0.1375	
	KLRK1 (NKG2D)	N/A	0.0286	0.0704	0.7049	1.9745	0.0000	0.0566	0.1506	1.1440	1.1440	0.0841	0.0286	0.0704	0.0841	0.2510	0.2750	0.2869	0.0000	0.1890	1.2327		
	ROR1	N/A	0.7312	0.0286	0.0000	0.3334	1.7570	3.8620	0.5460	1.6041	0.0704	1.2327	2.0496	4.0036	0.2630	1.4114	5.5097	0.0144	0.1506	0.0144	0.1506	3.6508	
	WT1	N/A	0.0144	0.0000	0.1243	0.1763	2.3190	2.1699	0.0286	1.4594	3.4370	0.1243	1.9964	3.9495	0.0000	2.9165	0.0841	4.6118	0.1635	0.0704	1.7137	1.5705	
	MET (C-Met)	N/A	2.7506	3.4222	1.5607	1.4803	6.2300	6.4411	4.7613	1.4699	0.5558	6.7623	6.2038	5.9873	4.4456	4.5844	4.8324	0.7740	6.1445	3.0036	5.0794	3.6450	
	CA9 (CAIX)	N/A	0.0144	0.2141	0.0000	0.0144	5.4877	0.8319	4.5336	0.5460	0.0000	0.0704	0.6229	0.0426	1.9782	2.1985	0.0426	0.0000	7.5568	0.1243	0.4222	2.0215	
	PROM1 (CD133)	N/A	0.0976	0.8074	0.0000	0.9411	0.0841	0.0841	0.0566	0.0841	0.0426	3.9079	0.0144	0.1506	0.0144	0.4542	0.1506	0.0704	0.1375	0.0286	0.0704	0.1110	
LICAM (CD171)	N/A	0.3896	0.8156	0.6229	0.1243	0.5753	2.3477	0.2141	5.6363	0.3334	2.7334	3.6769	8.2491	0.1375	4.1643	6.7570	0.5261	0.5361	4.3491	1.7004	6.8354		
CD70	N/A	6.9706	0.1635	7.4529	6.2919	6.8347	3.5361	0.0426	3.1619	0.8797	0.4114	1.4647	5.8202	0.0286	6.2223	0.1635	0.2750	5.2384	0.2016	0.5059	4.9621		
CEACAM5 (CEA)	N/A	0.1243	2.0670	0.0000	0.2265	0.0566	0.1890	0.2987	0.1635	0.1110	0.4222	1.4436	0.2388	1.4489	0.1110	2.1440	0.1110	0.0841	2.0704	0.4114	0.0704		
EGFR	N/A	0.1635	1.5410	0.0000	3.0790	4.2950	5.3459	3.9241	3.7159	0.2265	4.7634	4.8283	5.8497	1.4906	3.8012	0.2141	5.1085	0.2630	6.5534	2.1635			
EPCAM (Ep-CAM)	N/A	0.5361	7.4039	0.0000	0.6599	0.4222	2.9523	9.6185	8.5089	0.6323	8.3334	7.5399	4.2342	7.1480	0.7740	9.1172	0.8718	0.9336	8.4341	7.0353	3.6859		
EPHA2 (EphA2)	N/A	0.4854	2.2265	0.0000	0.3674	7.0611	5.7926	5.6488	5.5647	0.4114	6.3918	7.8590	7.9525	5.1094	5.9300	7.1738	0.4222	4.7698	3.3854	6.0027	6.0721		
FAP	N/A	0.0566	0.0704	0.0000	0.0144	0.1506	0.0566	0.0286	0.0144	0.2016	0.1506	0.0704	0.0144	0.4330	0.3561	0.0976	0.0704	5.2407	0.0566	0.0286	1.5059		
GPC3	N/A	0.0000	0.8400	0.0000	0.0000	0.1635	0.1375	0.4751	0.0841	0.0426	0.6135	0.1110	0.1110	0.0000	0.4222	0.6960	0.0000	0.0426	1.2388	0.6323	2.3646		
ERBB2 (HER2)	N/A	1.2510	10.5222	1.4647	3.3089	4.2510	4.2063	5.9669	3.6159	1.2449	4.7570	4.1102	4.2758	4.8435	4.5033	6.2246	1.5945	2.1890	5.5065	5.7578	5.4343		
IL13RA2 (IL13Ra2)	N/A	0.0566	0.0976	0.0000	0.0000	0.2265	0.0000	0.0000	0.0566	0.5361	0.0566	1.8400	0.0144	0.7312	9.0446	0.0000	0.1635	6.1183	0.0704	0.0566	0.0000		
FUT3 (LeY)	N/A	0.0144	0.1506	0.0566	0.0841	0.0000	0.0286	1.7442	0.0426	0.0426	0.1506	2.4222	0.0566	2.8875	0.0841	0.1763	0.0286	0.1110	0.1763	3.7560	0.1375		
MAGEA3	N/A	0.0704	0.0976	0.0000	0.1110	7.1033	0.8797	0.2750	0.0976	0.1110	7.0889	0.8953	0.1635	0.0286	7.3091	0.1243	4.3590	1.7949	0.2016	0.1110	4.4060		
MAGEA4	N/A	0.1243	0.0426	0.0000	0.1243	0.0000	0.1375	0.2265	0.2510	0.1375	0.2265	0.3561	0.2141	8.5461	9.6843	0.1506	0.2141	0.2750	0.1763	7.7173	6.0350		
MLANA (MART1)	N/A	0.3219	0.0286	0.1635	0.5619	0.3219	0.1506	0.3561	0.0000	0.0704	0.2016	0.1375	0.1243	0.1763	0.3896	0.2750	0.6135	0.4330	0.3103	0.5945	0.3896		
MSLN (Mesothelin)	N/A	0.1763	0.3103	0.0286	0.1506	0.1506	2.0807	0.4436	2.7929	0.2016	4.1043	1.7527	1.7991	0.0286	0.7049	5.7968	0.0841	0.2016	0.0976	1.6781	4.7296		
MUC1	N/A	0.1763	4.6616	0.0704	0.8953	1.2690	1.3448	1.6554	0.5753	1.7698	3.2750	4.4436	1.7181	1.9928	7.0095	3.7991	1.8875	5.1922	3.7602	3.3882			
MUC16	N/A	0.0144	0.0286	0.0144	3.4854	0.0144	0.0704	0.0426	0.1110	0.0144	0.0566	0.3334	0.5656	2.6668	0.0144	0.0426	0.4647	0.0704	1.4699	0.6599	0.0566		
CTAG1B (NY-ESO-1)	N/A	0.0426	0.1110	0.0000	0.1110	6.4000	0.0426	0.0976	0.0841	0.4222	0.0000	0.0426	0.0000	0.0426	5.9816	0.0000	0.0000	0.0000	0.0426	0.0976	0.3103		
CD274 (PD-L1)	N/A	0.7485	0.1506	3.6005	0.5160	5.0605	1.7866	1.2869	1.2810	0.2388	1.5607	2.5261	0.0976	2.5435	1.7698	1.3505	0.5460	2.8094	0.2630	2.9982	1.4005		
PSCA	N/A	0.3103	5.0700	0.1243	0.1763	1.5410	0.6323	0.0426	0.2987	0.0976	0.3674	1.9523	1.0704	6.4091	1.1243	1.4276	0.9855	2.8053	0.4854	1.3448	0.9411		
FOLH1 (PSMA)	N/A	0.0000	1.0976	0.0000	0.0976	0.4957	0.4114	0.0000	0.0000	0.0000	0.2750	0.2265	0.0286	0.0144	2.0670	0.0286	0.0000	0.0000	0.0566	1.1043	1.6323		
ROR1	N/A	0.7312	0.0286	0.0000	0.3334	1.7570	3.8620	0.5460	1.6041	0.0704	1.2327	2.0496	4.0036	0.2630	1.4114	5.5097	0.0144	0.1506	0.0144	0.1506	3.6508		
KDR (VEGFR2)	N/A	0.0000	0.0000	0.0286	0.0000	0.0976	0.0000	0.0000	0.0144	0.0976	0.0841	0.8875	0.0426	0.0000	2.1603	0.0000	3.0514	1.7782	0.0286	0.0000	0.0566		

Figure 1. Analysis of common hematologic and solid tumor CAR-T targets in selected cancer cell lines. Heat map of expression levels from the CCLE database for 12 hematological and 26 solid tumor CAR-T targets in 21 cancer lines with luciferase-expressing daughter lines available from ATCC. Values are log₂(TPM + 1). Values were gradiently color-coded by the Microsoft Excel software version 2308, with the midpoint (50th percentile) coded as white. Values above the midpoint were coded as red gradients. Values below the midpoint were coded as blue gradients. Note: WIL2-S did not have RNA-seq data within the CCLE database as indicated by N/A.

A

Cell Line Info	ATCC LUC2 ID	CRL-8885_E1	CRL-8885_E2	CRL-8885-LUC2_E1	CRL-8885-LUC2_E2	CCL-86-R1_E1	CCL-86-R1_E2	CCL-86-LUC2_E1	CCL-86-LUC2_E2
	Cell Line Name	WIL2-S	WIL2-S	WIL2-S-LUC2	WIL2-S-LUC2	RAJI	RAJI	RAJI-LUC2	RAJI-LUC2
	Lineage Subtype	B lymphoblast (ATCC)				Non Hodgkin Lymphoma (CCLE), B lymphocyte (ATCC)			
Haematological Tumor CAR Targets	TNFRSF17 (BCMA)	2.6034	2.5863	2.8300	2.5259	1.3341	0.9085	0.9724	1.5416
	IL3RA (CD123)	0.3835	0.4604	0.5875	0.6493	0.0000	0.0197	0.0000	0.0000
	SDC1 (CD138)	2.6672	2.6350	2.2521	2.1521	0.0000	0.0000	0.0000	0.0000
	CD19	4.7165	4.7405	4.5641	4.4393	6.7619	6.3809	6.6525	6.6966
	MS4A1 (CD20)	8.0526	8.0698	7.8880	7.8873	5.4484	6.1726	6.6860	6.6093
	CD22	7.4285	7.4467	6.9762	6.9798	5.1644	5.3359	6.2923	6.2771
	CD38	1.7122	1.5742	1.8423	1.9469	4.8609	5.7897	5.8123	5.7744
	CD5	0.0000	0.0000	0.0000	0.0000	0.0000	0.0000	0.0000	0.0000
	FUT3 (LeY)	0.0000	0.0000	0.0512	0.0000	0.0000	0.0000	0.0000	0.0000
	KLRK1 (NKG2D)	0.0000	0.0000	0.0000	0.0000	0.0000	0.0000	0.0000	0.0000
	ROR1	0.0000	0.0000	0.0000	0.0120	0.2722	0.9052	0.8378	0.8008
	WT1	0.0000	0.0000	0.0000	0.0000	0.0000	0.0000	0.0000	0.0000
	MET (C-Met)	0.0000	0.0000	0.0000	0.0000	1.0296	1.8161	2.7878	2.7289
	CA9 (CAIX)	0.0000	0.0000	0.0000	0.0000	0.0000	0.0000	0.0000	0.0000
	Solid Tumour CAR Targets	PROM1 (CD133)	0.0282	0.0000	0.0000	0.0000	0.0000	0.0000	0.0367
L1CAM (CD171)		0.0000	0.0000	0.0000	0.0000	0.0000	0.0000	0.0000	0.0000
CD70		7.1310	7.1892	7.1458	7.2590	7.6370	7.0802	6.4572	6.4472
CEACAM5 (CEA)		0.0000	0.0000	0.0000	0.0000	0.0000	0.0000	0.0000	0.0000
EGFR		0.0000	0.0000	0.0000	0.0000	0.0000	0.0000	0.0000	0.0000
EPCAM (Ep-CAM)		0.0000	0.1028	0.0000	0.0000	0.0000	0.0000	0.0000	0.0000
EPHA2 (EphA2)		0.0275	0.0000	0.0000	0.1871	0.0000	0.0000	0.0000	0.0000
FAP		0.0000	0.0000	0.0000	0.0000	0.0000	0.0000	0.0000	0.0000
GPC3		0.0000	0.0000	0.0000	0.0000	0.0000	0.0000	0.0000	0.0000
ERBB2 (HER2)		1.6341	1.5860	1.4579	1.4976	0.8825	0.7710	0.6043	0.6806
IL13RA2 (IL13Ra2)		0.0000	0.0000	0.0000	0.0000	0.0000	0.0000	0.0000	0.0000
FUT3 (LeY)		0.0000	0.0000	0.0512	0.0000	0.0000	0.0000	0.0000	0.0000
MAGEA3		0.0000	0.0000	0.0000	0.0000	0.0000	0.0000	0.0000	0.0000
MAGEA4		0.0000	0.0000	0.0000	0.0000	0.0000	0.0000	0.0000	0.0000
MLANA (MART1)		0.0000	0.0000	0.0000	0.0000	0.0000	0.0000	0.0000	0.0000
MSLN (Mesothelin)		0.0000	0.0000	0.0000	0.0000	0.0000	0.0000	0.0000	0.0000
MUC1		0.0000	0.2049	0.0000	0.0599	0.0000	0.0000	0.0763	0.0518
MUC16		0.0019	0.0000	0.0000	0.0000	0.0000	0.0209	0.0000	0.0000
CTAG1B (NY-ESO-1)		0.0000	0.0000	0.0000	0.0000	0.0000	0.0000	0.0000	0.0000
CD274 (PD-L1)		3.5061	3.5668	3.6920	3.7440	0.0774	0.0000	0.2622	0.1348
PSCA	0.0000	0.0000	0.0000	0.0000	0.0000	0.0000	0.0000	0.0000	
FOLH1 (PSMA)	0.0000	0.0000	0.0000	0.0000	0.0000	0.0000	0.0000	0.0000	
ROR1	0.0000	0.0000	0.0000	0.0120	0.2722	0.9052	0.8378	0.8008	
KDR (VEGFR2)	0.0000	0.0000	0.0000	0.0000	0.0000	0.0000	0.0000	0.0000	

B

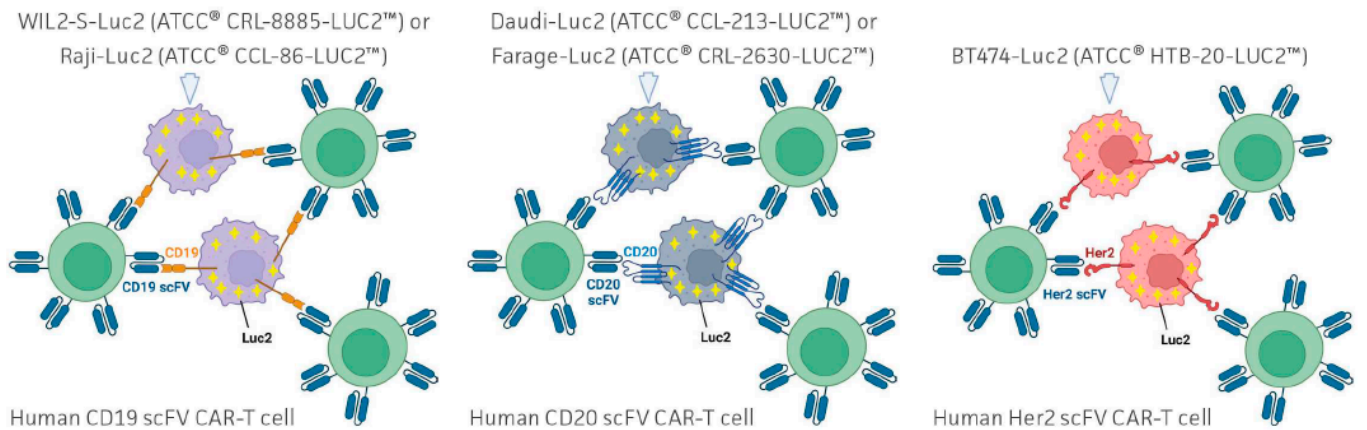


Figure 2. mRNA Seq analysis of common hematologic and solid tumor CAR-T targets in B lymphoblast and B lymphocyte cancer cell lines. (A) Heat map of RNA-seq data for 2 cancer cell lines

and 2 luciferase-expressing daughter cell lines showing expression levels of 12 hematologic tumor CAR-T targets and 26 solid tumor CAR-T targets. RNA sequencing was performed in duplicate by Psomogen. CD19 expression remains consistent pre- and post-luciferase transduction. Values are $\log_2(\text{FPKM} + 1)$. Values were gradiently color-coded by the Microsoft Excel software version 2308, with the midpoint (50th percentile) coded as white. Values above the midpoint were coded as red gradients. Values below the midpoint were coded as blue gradients. **(B)** Schematic showing CD19-positive WIL2-S-Luc2 and Raji-Luc2, CD20-positive Daudi-Luc2 and Farage-Luc2, and HER2-positive BT-474-Luc2 cells being surrounded and attacked by CD19-, CD20-, and HER2-targeting CAR-T cells, respectively. Created with BioRender.com (accessed on 7 October 2022).

3.2. Optimizing Ex Vivo CD19 CAR-T Cell-Mediated Cytotoxicity Assay Using Luminescence and Live Cell Imaging

To investigate whether the newly generated CAR-T luciferase reporter cell lines could be used to study the cytotoxic effects of antigen-specific CAR-T cells, we performed co-culture experiments using commercially available CAR-T cells specifically targeting CD19. CD19 CAR-T cells were paired with mock CAR-T control cells from the same donor. This allowed us to compare mock CAR-T cells and target-specific CAR-T cells in the same genetic background and with similar levels of non-specific killing activity. CD19-positive Raji-Luc2 cells or WIL2-S-Luc2 cells were co-cultured with either CD19 CAR-T or mock CAR-T cells at various ratios of CAR-T cells to target cells (1:1, 2:1, 5:1, and 10:1). After 24 h of co-culture, cell killing was measured via luminescence of the reporter cells. When the luminescence signal was normalized to wells containing only reporter cells, luminescence decreased with increasing amounts of CAR-T cells (Figure 3A,B). Importantly, luminescence decreased significantly more when reporter cells were co-cultured with CD19 CAR-T cells compared to non-specific levels of killing after co-culture with mock CAR-T cells. Overall, these results demonstrate how a reduction in luminescence in these reporter lines can be used as a proxy for CAR-T targeting efficacy.

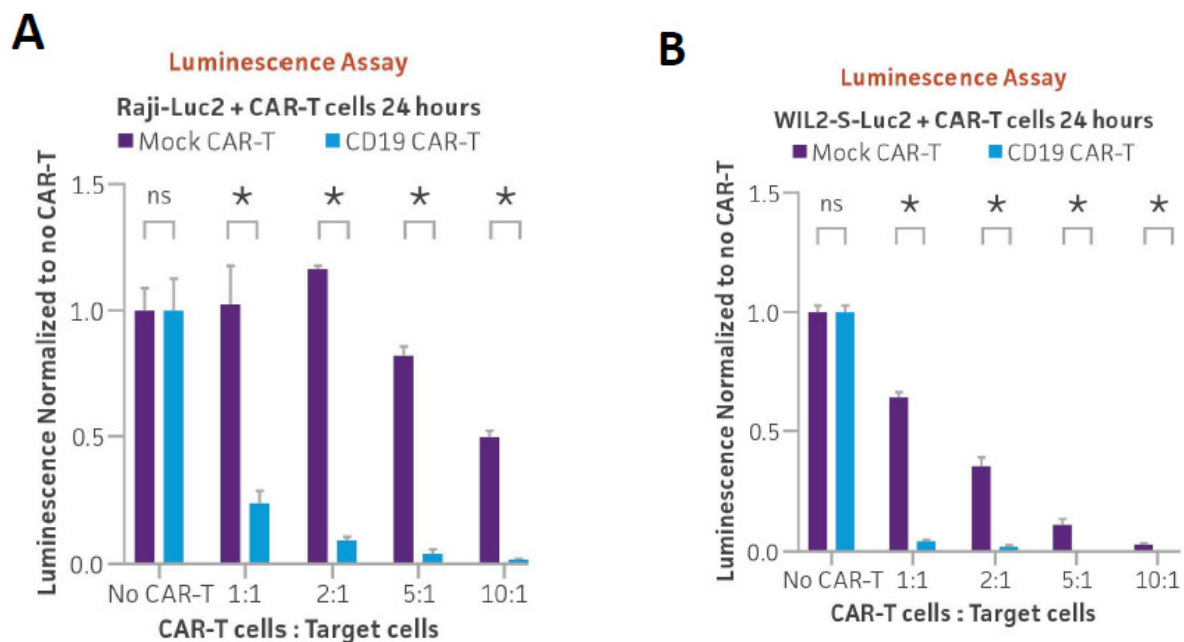


Figure 3. Cont.

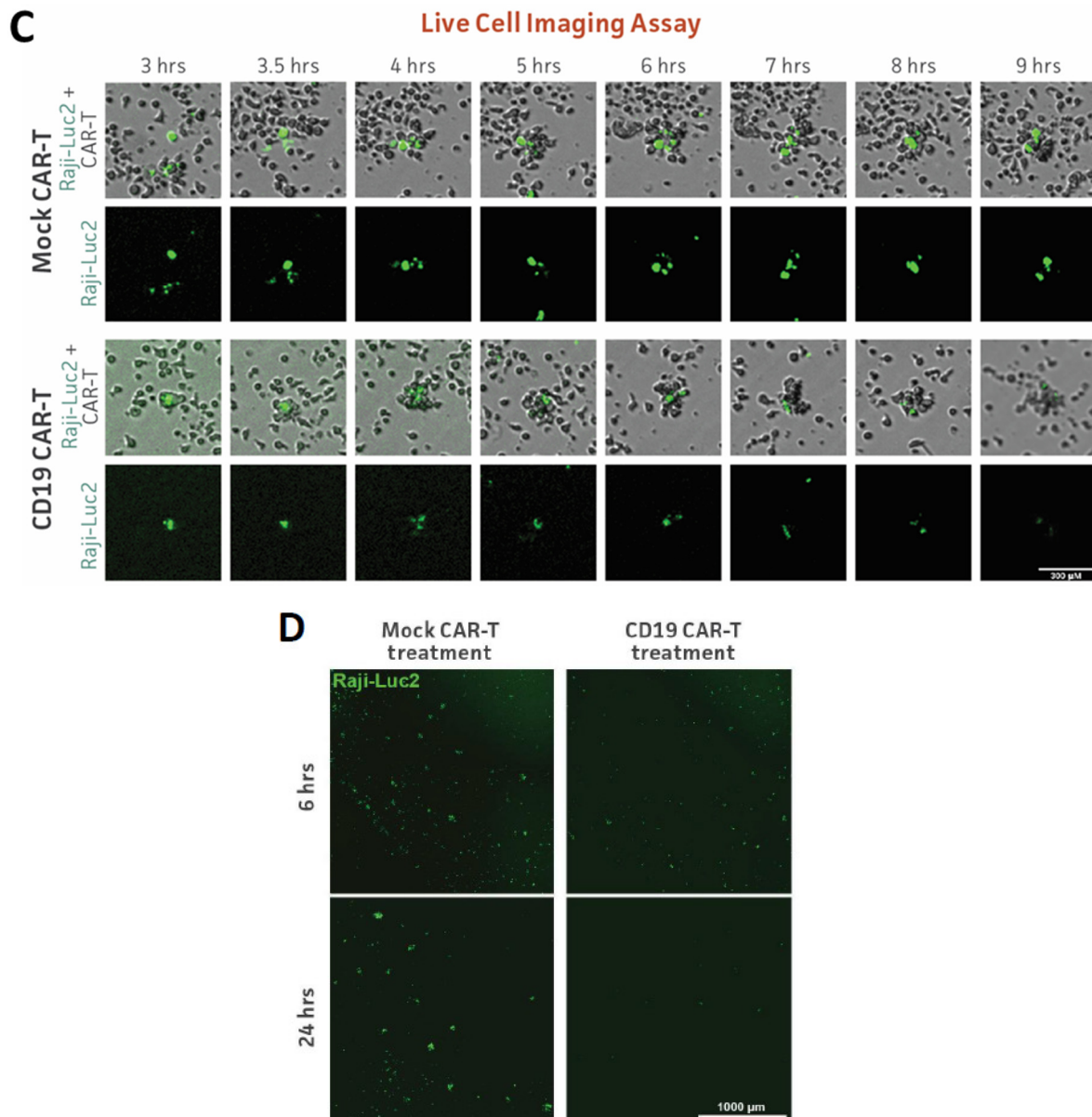


Figure 3. CD19 CAR-T in vitro killing assay of Raji-Luc2 and WIL2-S-Luc2 measured using luminescence and live cell imaging. (A) CD19-positive Raji-Luc2 cells (5×10^3) or (B) WIL2-S-Luc2 cells (5×10^3) were seeded into a 96-well plate and were used as target cells for either CD19 CAR-T or mock CAR-T cells (control) from the same donor, which were seeded at various ratios of CAR-T cells to target cells (1:1, 2:1, 5:1, and 10:1). After 24 h of co-culture, Bright-Glo reagent was added to the wells. Luminescence was read within 10 min using a plate reader and was normalized to wells with no CAR-T cells. * = significant difference and ns = not significant using an unpaired t test, with a single pooled variance. $N = 3$ in all experiments. * $p < 0.05$. (C) Raji-Luc2 cells were stained with Vybrant DiO dye, and real-time fluorescent images were captured every 30 min for 24 h during co-culture with either CD19 or mock CAR-T cells. Stained Raji-Luc2 cells (green) from the co-culture experiment were tracked for 6 h and became surrounded by CAR-T cells, resulting in a decrease in fluorescence when treated with CD19 CAR-T cells as compared to co-cultures with mock-CAR-T cells. Scale bar, 300 μm . (D) The larger fields of view of Vybrant DiO stained Raji-Luc2 cells (green) after 6 or 24 h of co-culture with either CD19 or mock CAR-T cells. Scale bar, 1000 μm .

While bioluminescence is a powerful and simple readout for cytotoxicity, it is not as convenient to monitor cell killing in real-time as fluorescence-based live cell imaging [19]. To evaluate CAR-T cytotoxicity using a real-time assay, Raji-Luc2 cells were stained with

lipophilic fluorescent DiO dye, and fluorescent images were captured every 30 min for 24 h during co-culture with either CD19 CAR-T cells or mock CAR-T cells. When Raji-Luc2 cells were co-cultured with mock CAR-T cells, fluorescence levels decreased slowly and remained relatively constant, even as the reporter cells became surrounded by CAR-T cells. However, a quick decrease in fluorescence, indicating the massive killing of target cells, was observed when stained Raji-Luc2 cells were co-cultured with CD19 CAR-T cells (Figure 3C; Videos S1 and S2). Visualizing a large field of cells displayed a significant fluorescence decrease observed at 24 h after co-culture with CD19 CAR-T cells, while no significant change in fluorescence was observed after co-culture with mock CAR-T cells (Figure 3D). These results indicate that the CAR-T target reporter lines can be used to monitor CAR-T cell targeting using fluorescence-based live imaging techniques in addition to bioluminescence.

3.3. Optimizing Ex Vivo HER2 CAR-T Cell-Mediated Cytotoxicity Assay Using Luminescence and xCELLigence Live Cell Assay in Adherent Cells

Improving the efficacy of CAR-T cells on solid tumors remains an active area of research [20]. To investigate whether the BT-474-Luc2 line could be used as a reporter of HER2 CAR-T cell targeting, the cytotoxicity of HER2 CAR-T cells on BT-474-Luc2 cells was measured by luminescence. HER2-positive BT-474-Luc2 cells were seeded at the same CAR-T to target cell ratios as above using either HER2 CAR-T or mock CAR-T cells. After 24 h of co-culture, luminescence dramatically decreased with increasing doses of HER2 CAR-T cells (Figure 4A). This result demonstrates that the BT-474-Luc2 reporter line can be used to monitor HER2 CAR-T cell targeting via luminescence.

As the only adherent line generated in this study, BT-474-Luc2 targeting by HER2 CAR-T cells could also be tested using the impedance assay. In this assay, as effector cells kill adherent cells and they detach from the plate, electrical resistance in the co-culture decreases [21]. BT-474-Luc2 cells alone or co-cultured with mock CAR-T cells at a 10:1 CAR-T to target cell ratio did not cause a change in cell impedance over time. However, when BT-474-Luc2 cells were co-cultured with HER2 CAR-T cells, impedance dramatically decreased, indicating the detachment of BT-474-Luc2 cells from the plate (Figure 4B). Taken together, these results show that the BT-474-Luc2 line can be used to monitor HER2 CAR-T targeting efficacy either by luminescence or in real-time by impedance.

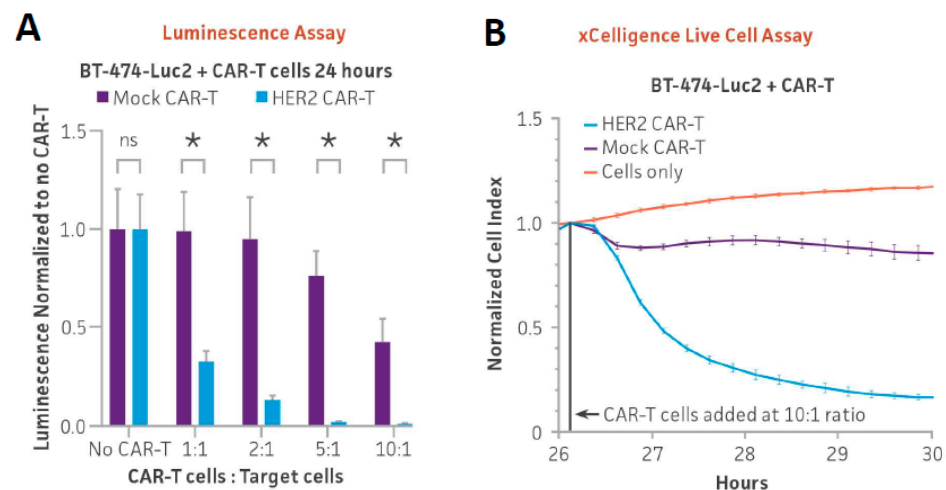


Figure 4. Cont.

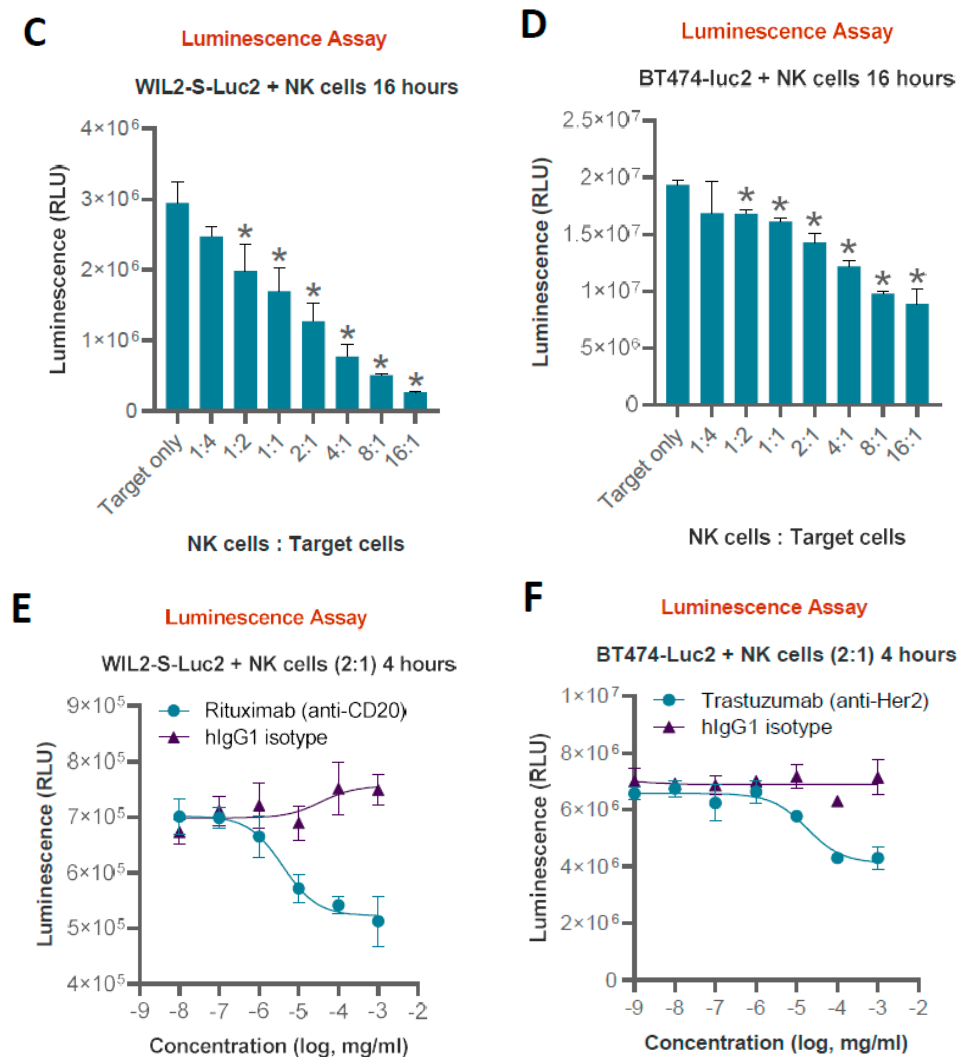


Figure 4. BT-474-Luc2 and WIL2-S-Luc2 used in CAR-T and NK cytotoxicity assays. (A) HER2-positive BT-474-Luc2 cells (5×10^3) were seeded into a 96-well plate, and either HER2 CAR-T or mock CAR-T cells were added at various ratios of CAR-T cells to target cells (1:1, 2:1, 5:1, and 10:1). (B) HER2 CAR-T cells were used to target 2×10^4 HER2-positive BT-474-Luc2 cells at a 10:1 ratio, and cell killing was measured using the xCELLigence system. Mock CAR-T cells from the same donor were used as a control. (C) WIL2-S-Luc2 cells or (D) BT-474-Luc2 cells were co-cultured with NK cells for 16 h at various NK to target cell ratios (1:4, 1:2, 1:1, 2:1, 4:1, 8:1, and 16:1) after which luciferase activity was measured. (E) Antibody-dependent cell-mediated cytotoxicity (ADCC) assay using Rituximab (anti-CD20) with WILS-2-Luc2 cells or (F) Trastuzumab (anti-HER2) monoclonal antibodies with BT474-Luc2 cells. Concentrations of monoclonal antibody or IgG1 control varying from 10 pg to 1 μ g/mL were added to co-cultures of primary NK cells and reporter cells at a 2:1 NK/target cell ratio. Luminescence was measured after 4 h of co-culture. * = significant difference and ns = not significant using an unpaired t test, with a single pooled variance. $N = 3$ in all experiments. * $p < 0.05$.

3.4. Using Luminescence as a Readout for Ex Vivo NK Direct Killing and ADCC

Another important area of cancer therapy research, in addition to CAR-T therapy, is the use of monoclonal antibodies [22]. Next, we evaluated the ability of two of the luciferase lines, WIL2-S-Luc2 and BT-474-Luc2, to serve as reporters of antibody-dependent cellular cytotoxicity. First, we conducted a direct killing assay using primary NK cells at varying NK-to-target cell ratios. After 16 h of co-culture, luminescence dramatically decreased with increasing ratios of NK to target cells, indicating dose-dependent reporter cell killing

by NK cells (Figure 4C,D). Using an NK-to-target cell ratio of 2:1, we next performed the luciferase assay with anti-CD20 and anti-HER2 antibodies for NK cell-mediated ADCC (antibody-dependent cell-mediated cytotoxicity) against Wil2-S-Luc2 and BT-474-Luc2 cells, respectively. Rituximab (anti-CD20) or Trastuzumab (anti-HER2) monoclonal antibodies were administered at various concentrations using IgG1 as an isotype control. We observed a dose-dependent decrease in luciferase signal relative to IgG1-treated controls in WIL2-S-Luc2 and BT-474-Luc2 cells, indicating antibody-dependent cell killing (Figure 4E,F). This result demonstrates that these reporter lines can also be targeted by monoclonal antibodies and thus can be used to measure antibody-mediated cellular cytotoxicity.

3.5. Optimizing Ex Vivo CD20 CAR-T Cell-Mediated Cytotoxicity Assay Using Luminescence and Cytotox Red Dye-Based Live Cell Imaging

Finally, we investigated whether the engineered Farage-Luc2 and Daudi-Luc2 lines could serve as reporters of CD20 CAR-T targeting. CD20-positive Farage-Luc2 cells or Daudi-Luc2 cells were co-cultured with either CD20 CAR-T or mock CAR-T cells at various ratios of CAR-T cells to target cells (1:1, 2:1, 5:1, and 10:1). After 24 h, luminescence significantly decreased following co-culture with CD20 CAR-T cells relative to mock CAR-T controls as seen for the other luciferase lines (Figures 5A and 6A). We then used a tractable live imaging approach to assess cell death of the reporter lines after co-culture with CD20 CAR-T cells. Cytotox red, which only stains dead cells [23], was added to co-cultures of each reporter line with either CD20 CAR-T cells or mock CAR-T cells at various ratios of CAR-T to target cells. Red fluorescence was then quantified after 24 h of co-culture. While there was a slight increase in red fluorescence after co-culture with mock CAR-T cells, a dramatic and dose-dependent increase in red fluorescence intensity was observed after co-culture with CD20 CAR-T cells for both Farage-Luc2 and Daudi-Luc2 (Figures 5B and 6B). Live cell imaging of the co-cultures revealed a significant increase in red fluorescence over time in Farage-Luc2 or Daudi-Luc2 cells co-cultured with CD20 CAR-T cells compared to reporter cells co-cultured with mock CAR-T cells (Figures 5C,D and 6C,D; Videos S3–S6). These results indicate elevated levels of targeted cell killing of both reporter lines, specifically by CD20 CAR-T cells, and demonstrate another live imaging approach that can be used in parallel with luminescence.

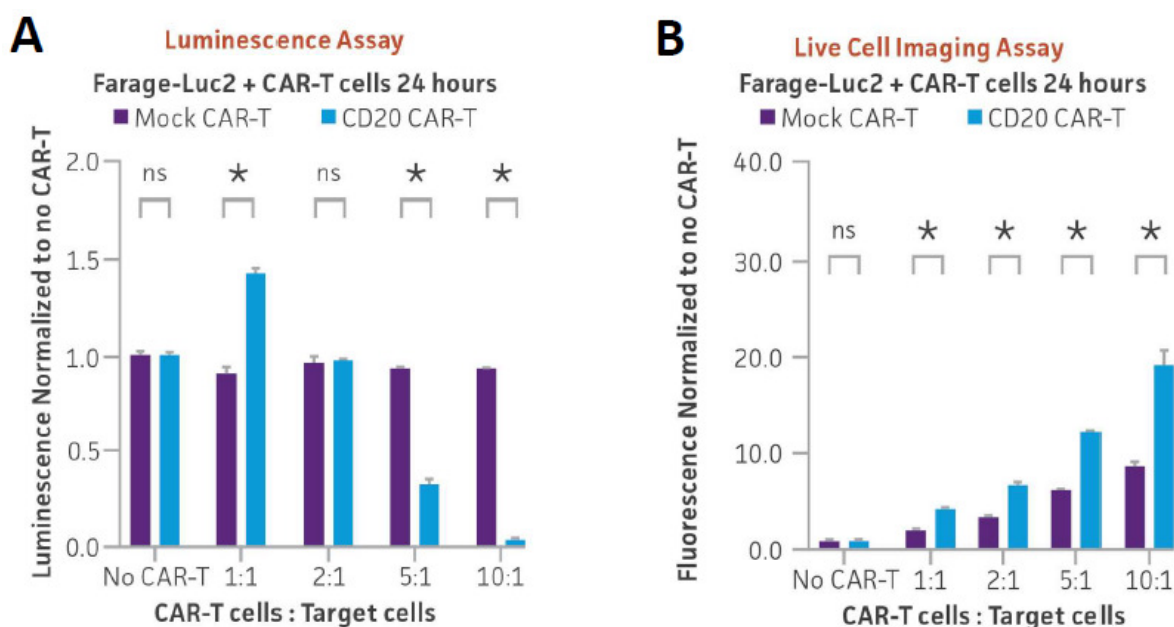


Figure 5. Cont.

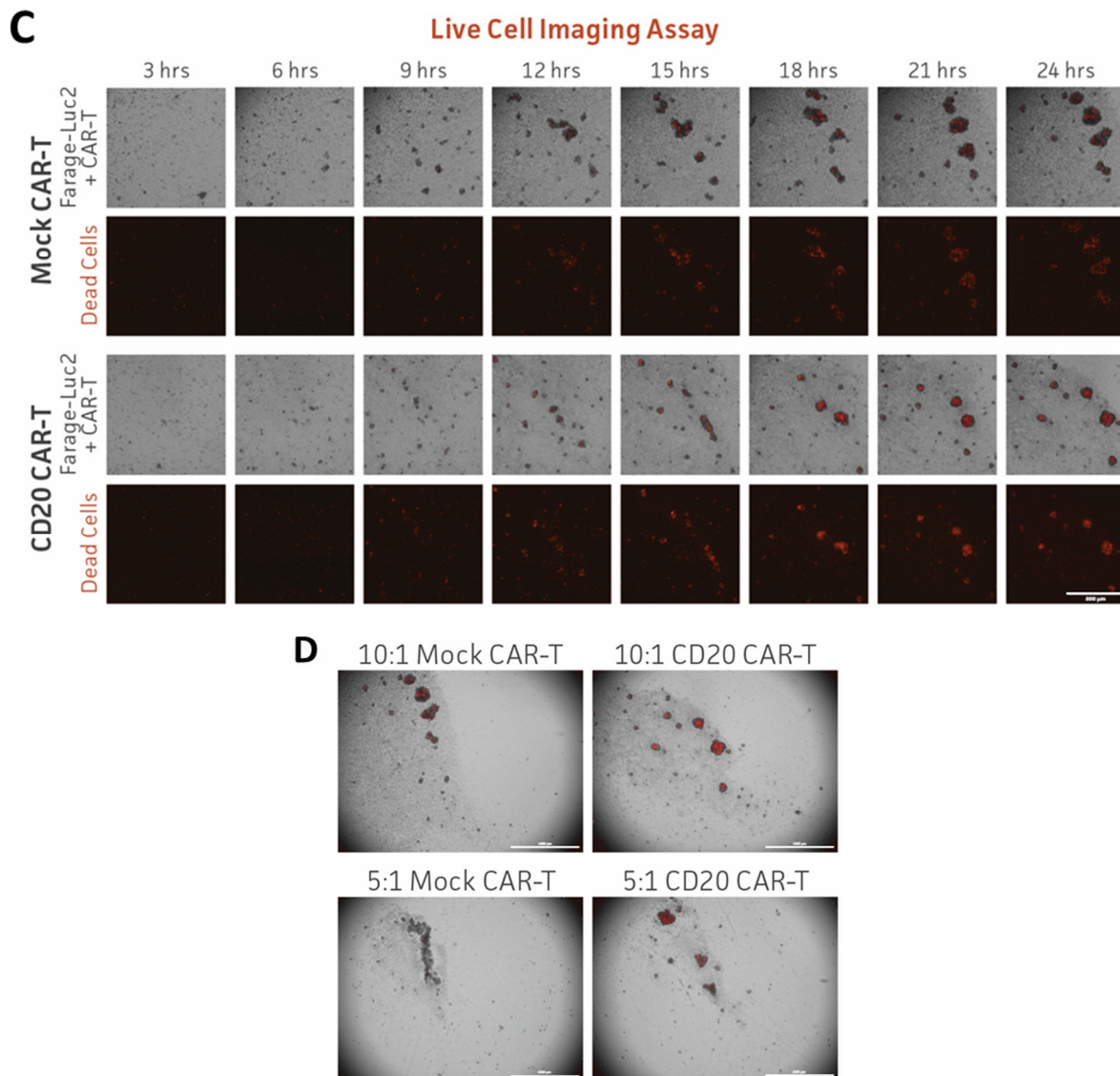


Figure 5. CD20 CAR-T in vitro killing assay of Farage-Luc2 measured using luminescence and live cell imaging. (A) CD20-positive Farage-Luc2 cells (5×10^3) were seeded into a 96-well plate, and CD20 CAR-T or mock CAR-T cells were added at various ratios of CAR-T to target cells (1:1, 2:1, 5:1, and 10:1). (B) Farage-Luc2 cells (5×10^3) were co-cultured with CD20 CAR-T cells or mock CAR-T cells in the presence of Incucyte Cytotox red dye. Fluorescent images were captured every hour for 24 h, and red fluorescence was quantified and plotted. * = significant difference and ns = not significant using an unpaired t test, with a single pooled variance. $N = 3$ in all experiments. * $p < 0.05$. (C) Series of images captured during Farage-Luc2 cells co-culture with CD20 or mock CAR-T cells in the presence of Cytotox Red. Scale bar, 300 μm . (D) The larger fields of view of Farage-Luc2 cells co-culture with CD20 or mock CAR-T cells in the presence of Cytotox Red at 24 h. Scale bar, 1000 μm .

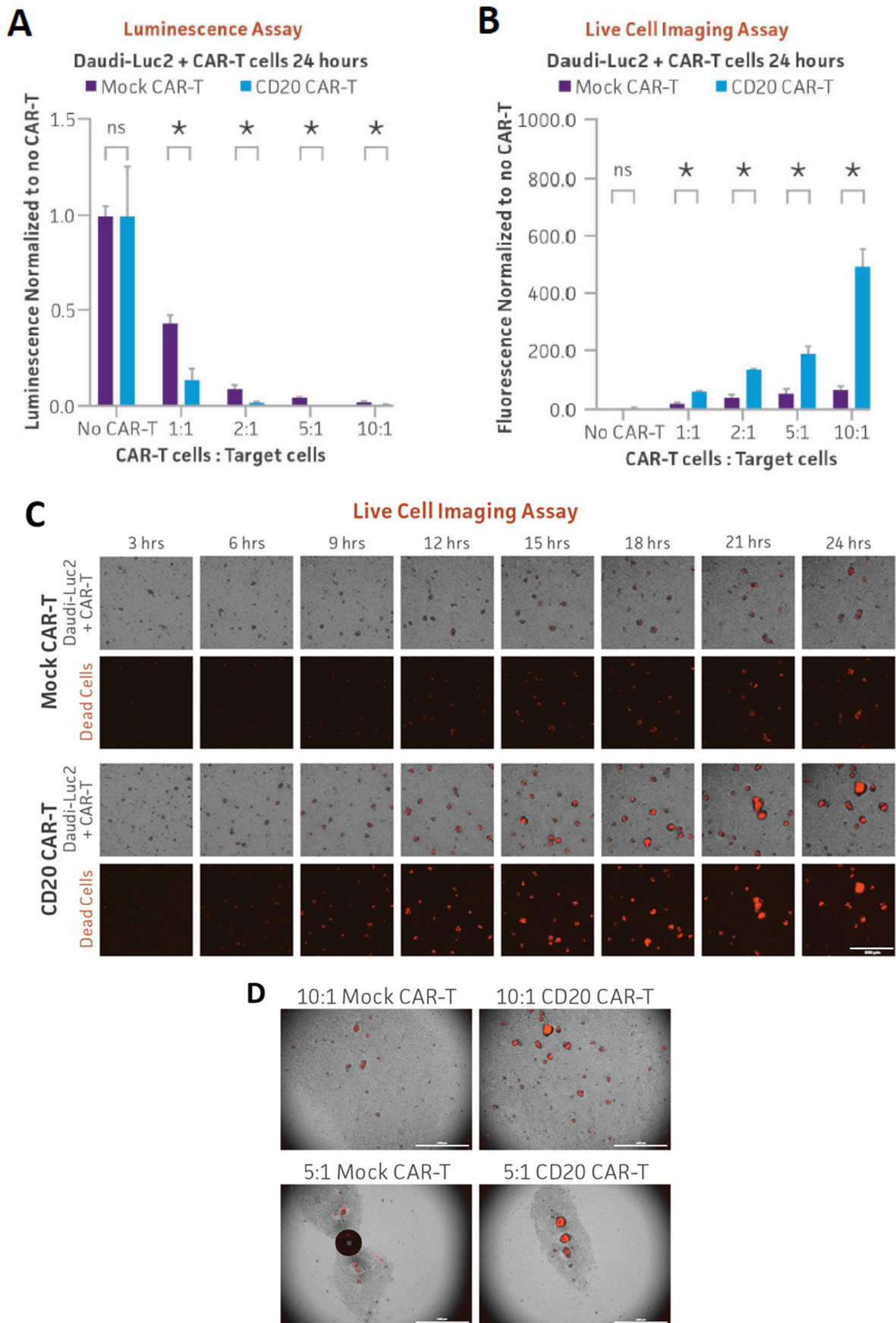


Figure 6. CD20 CAR-T in vitro killing assay of Daudi-Luc2 measured using luminescence and live cell imaging. (A) CD20-positive Daudi-Luc2 cells (5×10^3) were seeded into a 96-well plate, and CD20

CAR-T or mock CAR-T cells were added at various ratios of CAR-T cells to target cells (1:1, 2:1, 5:1, and 10:1). After 24 h of co-culture, Bright-Glo was added to the wells and luminescence was measured. (B) Daudi-Luc2 cells (5×10^3) were co-cultured with CD20 CAR-T cells or mock CAR-T cells in the presence of Incucyte Cytotox red dye. Fluorescent images were captured every hour for 24 h, and red fluorescence was quantified and plotted. * = significant difference and ns = not significant using an unpaired t test, with a single pooled variance. $N = 3$ in all experiments. * $p < 0.05$. (C) Series of images captured during Daudi-Luc2 cells co-culture with CD20 or mock CAR-T cells in the presence of Cytotox Red. Scale bar, 300 μm . (D) The larger fields of view of Daudi-Luc2 cells co-culture with CD20 or mock CAR-T cells in the presence of Cytotox Red at 24 h. Scale bar, 1000 μm .

4. Discussion

In this study, we generated five luciferase reporter cancer cell lines and demonstrated their use in a variety of multimodality imaging approaches to measure CAR-T cell cytotoxicity. The CAR-T target luciferase reporter tumor cell lines that we engineered were derived from a variety of highly malignant liquid and solid cancer types, namely B cell lymphoma, Burkitt's lymphoma, Non-Hodgkin's B cell lymphoma, and ductal breast carcinoma. These novel target cell lines were generated from parental tumor cells that have high endogenous expression of target antigens such as CD19, CD20, and HER2. Stable luciferase-expressing clones were engineered to display high signal-to-noise ratios, aiding in the interpretation of the data. Furthermore, authenticating these cell lines using tried and true methods such as short tandem repeat (STR) profiling, mycoplasma detection, cell growth rate, and morphology assays can satisfy the requirements for authentication set by regulatory bodies and give researchers further confidence in their experimental results. The performance of the CAR-T target luciferase reporter cell lines was verified in T cell co-culture experiments. Commercially available CAR-T cells targeting CD19, CD20, and HER2 were employed in this study, with which non-targeting mock CAR-T cells from the same donor were paired as controls. The cytotoxicity of the CAR-T cells against target tumor cells was measured using a luciferase assay, a commercially available impedance assay, and two different fluorescent live imaging assays. Our results demonstrate that the luciferase reporter system is a simple, robust, and highly sensitive means to measure biological processes in cancer and T cell ex vivo co-cultures through a variety of multimodality imaging methods.

Assays currently in use have various drawbacks (Table 1). Unlike the luminescence and live imaging assays, the chromium–release assay uses radioactive isotopes that can pose safety concerns and require specialized handling and disposal procedures. The assay also only provides a single-time-point measurement and does not allow for real-time or kinetic assessment of CAR-T cell cytotoxicity over time [11,21] as live imaging allows. Some background release of chromium can occur even in the absence of CAR-T cells, leading to false-positive results and potentially affecting the accuracy of the assay [8,11,12]. Further, the chromium–release assay may not be sensitive enough to detect low levels of target cell killing, especially when CAR-T cells are present in limited numbers or exhibit lower cytotoxic activity [8]. As demonstrated previously, the luciferase assay is highly sensitive [24,25]. We further show here that a reduction in luminescence can be detected even at low ratios of effector to target cells. The chromium–release assay requires physical contact between effector CAR-T cells and target cells to measure cytotoxicity accurately. However, certain CAR-T cell constructs or target cells may have limited adhesion capabilities or poor compatibility, leading to reduced accuracy or underestimation of cytotoxicity. Moreover, the chromium–release assay requires time for the released chromium to be measured, which introduces a delay between target cell lysis and data acquisition [11]. This delay may not capture the full kinetics of CAR-T cell cytotoxicity and can impact the accuracy of time-sensitive measurements. The luciferase assay avoids this delay before lysis, as data are acquired within minutes.

Table 1. Comparison of cell-mediated cytotoxicity assays.

	Chromium Release	Bioluminescence Imaging	Impedance	Flow Cytometry	Fluorescence Imaging–Cell Labeling	Fluorescence Imaging–Cytotox Dye in Media
Principal measure of cytotoxicity	⁵¹ Cr release	Luciferase activity	Cell detachment	Live/dead staining phenotype	Decrease in fluorescent signal	Dye infiltration into dead cell
Radioactive materials needed	Yes	No	No	No	No	No
Target cell labeling required	Yes	No	No	Yes	Yes	No
Genetic modification of target cells	No	Yes (reporter gene)	No	No	No	No
Endpoint/kinetic	Endpoint	Temporal & Spatial	Temporal	Endpoint	Temporal & Spatial	Temporal & Spatial
Real-time measurement	No	Yes	Yes	No	Yes	Yes
Maximum time point measured	18–24 h	Days	Days	Days	Days	Days
Ability to measure different cytotoxicity heterogenous targets	No	No	No	Yes	Yes	Yes
Throughput and automatability	Low	High	High	High	High	High

Impedance-based assays typically measure overall changes in electrical impedance and cannot distinguish between CAR-T cell-mediated cytotoxicity and non-specific effects, such as changes in cell adherence or morphology, which live imaging can capture. Impedance assays may lack the sensitivity to detect low levels of target cell killing, especially when CAR-T cells are present in small numbers or have lower cytotoxic potential. As mentioned above, the luciferase assay can detect a decrease in signal even at low effector-to-target cell ratios. Impedance-based assays are often limited to measuring a single parameter at a time and may not easily allow for multiplexing or simultaneous evaluation of multiple aspects of CAR-T cell cytotoxicity. Furthermore, impedance-based assays measure changes in electrical impedance caused by cellular interactions but do not directly measure cytotoxicity [26]. Changes in impedance may be influenced by factors other than cytotoxicity, such as changes in cell adherence, morphology, or cell viability [27]. This lack of direct measurement of cytotoxicity can introduce some degree of uncertainty and affect the accuracy of the assay. While both the luciferase and live imaging assays require labeling, any changes in luminescence or fluorescence are a direct result of cell death. Further, impedance-based assays may have a limited ability to detect low levels of target cell killing or discriminate between different degrees of cytotoxicity. This limitation can lead to underestimation of CAR-T cell activity when cytotoxicity is low or subtle, which is more likely to be captured by the quantitative sensitivity of the luciferase assay and continual monitoring by live imaging.

Lastly, flow cytometry assays may have a limited dynamic range, making it challenging to accurately measure high levels of target cell killing or discriminate between different degrees of cytotoxicity [28]. Flow cytometry provides information on individual cells but does not provide spatial information about the interactions between CAR-T cells and target cells within the tumor microenvironment [29]. A major strength of the live imaging assay is the ability to capture these interactions. Non-specific binding of antibodies or detection reagents to cells can introduce background noise, potentially impacting the accuracy of the assay and leading to false-positive or false-negative results. Furthermore, flow cytometry assays rely on fluorophore-labeled antibodies for target cell detection. The choice of fluorophores

can impact the accuracy and sensitivity of the assay. Some fluorophores may have limited brightness, photobleaching, or spectral overlap, leading to decreased detection sensitivity or potential interference with other fluorescence channels [30]. Non-specific binding of antibodies or detection reagents to cells can generate false-positive results, particularly when dealing with low-level antigen expression on non-target cells. This non-specific binding can result in overestimation of CAR-T cell cytotoxicity or false identification of target cells. While the luciferase assay necessitates genetic modification and live imaging requires labeling via dyes, these labels are highly specific to the target cells, avoiding many of these drawbacks. Moreover, flow cytometry assays primarily focus on surface marker expression or cell death markers, but they may not capture other phenotypic changes or functional alterations in CAR-T cells that could affect their cytotoxic potential.

5. Conclusions

Overall, the luminescence assay's quantitative power, coupled with kinetic insights from live imaging, renders these multimodality imaging assays highly efficient for real-time monitoring of ex vivo CAR-T cell-mediated cytotoxicity. While each CAR-T cytotoxicity assay has inherent limitations, utilizing luciferase reporter CAR-T target tumor cell lines in combined multimodality imaging assays creates an optimized platform to facilitate the collection of more comprehensive cell information during CAR-T-mediated tumor cell elimination. The generated cell lines, along with other ATCC luciferase tumor cell lines expressing key CAR-T targets, serve as valuable and reliable tools for evaluating CAR-T targeting efficacy in the advancement of enhanced CAR-T therapies.

Supplementary Materials: The following supporting information can be downloaded at: <https://www.mdpi.com/article/10.3390/cancers16142497/s1>, Figure S1: Characterization of CAR-T target cell lines: Cell Morphology; Figure S2: Characterization of CAR-T target cell lines: Growth Curve; Figure S3: Characterization of CAR-T target cell lines: Antigen FACS analysis; Figure S4: Characterization of CAR-T target cell lines: Luciferase assay; Figure S5: Characterization of CAR-T target cell lines: Luciferase activity stability; Videos S1 and S2: CD19 CAR-T in vitro killing assay of Raji-Luc2 measured using live cell imaging; Videos S3 and S4: CD20 CAR-T in vitro killing assay of Farage-Luc2 measured using live cell imaging; Videos S5 and S6: CD20 CAR-T in vitro killing assay of Daudi-Luc2 measured using live cell imaging.

Author Contributions: Conceptualized the project and designed the methodology, J.G.F., F.T. and Z.G.; Performed experiments, analyzed data, and contributed to writing the manuscript, J.G.F., L.C., H.C. and C.E.M.; Supervised all aspects of the project and wrote the manuscript, F.T. and Z.G.; All authors have read and agreed to the published version of the manuscript.

Funding: This research received no external funding.

Institutional Review Board Statement: Not applicable.

Informed Consent Statement: Not applicable.

Data Availability Statement: The data presented in this study are available on request from the corresponding author.

Acknowledgments: We thank Haiyun Liu and Alicia Walker for their experimental helps during the preliminary study phase. We thank Brian Shapiro, Cara Wilder, and Lucas Altenbaumer for helping edit and review the manuscript. We thank Andrew Burke for optimizing the figures and graphs.

Conflicts of Interest: The authors declare no conflicts of interest.

References

1. June, C.H.; O'Connor, R.S.; Kawalekar, O.U.; Ghassemi, S.; Milone, M.C. CAR T cell immunotherapy for human cancer. *Science* **2018**, *359*, 1361–1365. [[CrossRef](#)] [[PubMed](#)]
2. Sadelain, M.; Brentjens, R.; Riviere, I. The basic principles of chimeric antigen receptor design. *Cancer Discov.* **2013**, *3*, 388–398. [[CrossRef](#)] [[PubMed](#)]
3. Porter, D.L.; Levine, B.L.; Kalos, M.; Bagg, A.; June, C.H. Chimeric antigen receptor-modified T cells in chronic lymphoid leukemia. *N. Engl. J. Med.* **2011**, *365*, 725–733. [[CrossRef](#)]

4. Kochenderfer, J.N.; Wilson, W.H.; Janik, J.E.; Dudley, M.E.; Stetler-Stevenson, M.; Feldman, S.A.; Maric, I.; Raffeld, M.; Nathan, D.A.; Lanier, B.J.; et al. Eradication of B-lineage cells and regression of lymphoma in a patient treated with autologous T cells genetically engineered to recognize CD19. *Blood* **2010**, *116*, 4099–4102. [[CrossRef](#)]
5. Garfall, A.L.; Maus, M.V.; Hwang, W.T.; Lacey, S.F.; Mahnke, Y.D.; Melenhorst, J.J.; Zheng, Z.; Vogl, D.T.; Cohen, A.D.; Weiss, B.M.; et al. Chimeric Antigen Receptor T Cells against CD19 for Multiple Myeloma. *N. Engl. J. Med.* **2015**, *373*, 1040–1047. [[CrossRef](#)]
6. Sengsayadeth, S.; Savani, B.N.; Oluwole, O.; Dholaria, B. Overview of approved CAR-T therapies, ongoing clinical trials, and its impact on clinical practice. *EJHaem* **2022**, *3*, 6–10. [[CrossRef](#)]
7. Jackson, H.J.; Rafiq, S.; Brentjens, R.J. Driving CAR T-cells forward. *Nat. Rev. Clin. Oncol.* **2016**, *13*, 370–383. [[CrossRef](#)] [[PubMed](#)]
8. Kiesgen, S.; Messinger, J.C.; Chintala, N.K.; Tano, Z.; Adusumilli, P.S. Comparative analysis of assays to measure CAR T-cell-mediated cytotoxicity. *Nat. Protoc.* **2021**, *16*, 1331–1342. [[CrossRef](#)] [[PubMed](#)]
9. Brunner, K.T.; Mael, J.; Cerottini, J.C.; Chapuis, B. Quantitative assay of the lytic action of immune lymphoid cells on 51-Cr-labelled allogeneic target cells in vitro; inhibition by isoantibody and by drugs. *Immunology* **1968**, *14*, 181–196. [[PubMed](#)]
10. Erskine, C.L.; Henle, A.M.; Knutson, K.L. Determining optimal cytotoxic activity of human Her2neu specific CD8 T cells by comparing the Cr51 release assay to the xCELLigence system. *J. Vis. Exp.* **2012**, e3683. [[CrossRef](#)]
11. Peper, J.K.; Schuster, H.; Loffler, M.W.; Schmid-Horch, B.; Rammensee, H.G.; Stevanovic, S. An impedance-based cytotoxicity assay for real-time and label-free assessment of T-cell-mediated killing of adherent cells. *J. Immunol. Methods* **2014**, *405*, 192–198. [[CrossRef](#)] [[PubMed](#)]
12. Riss, T.; Niles, A.; Moravec, R.; Karassina, N.; Vidugiriene, J. Cytotoxicity Assays: In Vitro Methods to Measure Dead Cells. In *Assay Guidance Manual*; Markossian, S., Grossman, A., Brimacombe, K., Arkin, M., Auld, D., Austin, C., Baell, J., Chung, T.D.Y., Coussens, N.P., Dahlin, J.L., et al., Eds.; Eli Lilly & Company and the National Center for Advancing Translational Sciences: Bethesda, MD, USA, 2019; pp. 379–394.
13. Karimi, M.A.; Lee, E.; Bachmann, M.H.; Salicioni, A.M.; Behrens, E.M.; Kambayashi, T.; Baldwin, C.L. Measuring cytotoxicity by bioluminescence imaging outperforms the standard chromium-51 release assay. *PLoS ONE* **2014**, *9*, e89357. [[CrossRef](#)] [[PubMed](#)]
14. Chu, F.; Cao, J.; Neelalpu, S.S. Versatile CAR T-cells for cancer immunotherapy. *Contemp. Oncol.* **2018**, *22*, 73–80. [[CrossRef](#)] [[PubMed](#)]
15. Martinez, M.; Moon, E.K. CAR T Cells for Solid Tumors: New Strategies for Finding, Infiltrating, and Surviving in the Tumor Microenvironment. *Front. Immunol.* **2019**, *10*, 128. [[CrossRef](#)] [[PubMed](#)]
16. Cappell, K.M.; Kochenderfer, J.N. Long-term outcomes following CAR T cell therapy: What we know so far. *Nat. Rev. Clin. Oncol.* **2023**, *20*, 359–371. [[CrossRef](#)] [[PubMed](#)]
17. Budi, H.S.; Ahmad, F.N.; Achmad, H.; Ansari, M.J.; Mikhailova, M.V.; Suksatan, W.; Chupradit, S.; Shomali, N.; Marofi, F. Human epidermal growth factor receptor 2 (HER2)-specific chimeric antigen receptor (CAR) for tumor immunotherapy; recent progress. *Stem Cell Res. Ther.* **2022**, *13*, 40. [[CrossRef](#)] [[PubMed](#)]
18. Gazzano-Santoro, H.; Ralph, P.; Ryskamp, T.C.; Chen, A.B.; Mukku, V.R. A non-radioactive complement-dependent cytotoxicity assay for anti-CD20 monoclonal antibody. *J. Immunol. Methods* **1997**, *202*, 163–171. [[CrossRef](#)] [[PubMed](#)]
19. Tung, J.K.; Berglund, K.; Gutekunst, C.A.; Hochgeschwender, U.; Gross, R.E. Bioluminescence imaging in live cells and animals. *Neurophotonics* **2016**, *3*, 025001. [[CrossRef](#)] [[PubMed](#)]
20. Dagar, G.; Gupta, A.; Masoodi, T.; Nisar, S.; Merhi, M.; Hashem, S.; Chauhan, R.; Dagar, M.; Mirza, S.; Bagga, P.; et al. Harnessing the potential of CAR-T cell therapy: Progress, challenges, and future directions in hematological and solid tumor treatments. *J. Transl. Med.* **2023**, *21*, 449. [[CrossRef](#)] [[PubMed](#)]
21. Lisby, A.N.; Carlson, R.D.; Baybutt, T.R.; Weindorfer, M.; Snook, A.E. Evaluation of CAR-T cell cytotoxicity: Real-time impedance-based analysis. *Methods Cell Biol.* **2022**, *167*, 81–98. [[CrossRef](#)] [[PubMed](#)]
22. Lo Nigro, C.; Macagno, M.; Sangiolo, D.; Bertolaccini, L.; Aglietta, M.; Merlano, M.C. NK-mediated antibody-dependent cell-mediated cytotoxicity in solid tumors: Biological evidence and clinical perspectives. *Ann. Transl. Med.* **2019**, *7*, 105. [[CrossRef](#)] [[PubMed](#)]
23. Schwietzer, Y.A.; Susek, K.H.; Chen, Z.; Alici, E.; Wagner, A.K. A tractable microscopy- and flow cytometry-based method to measure natural killer cell-mediated killing and infiltration of tumor spheroids. *Methods Cell Biol.* **2023**, *178*, 43–61. [[CrossRef](#)] [[PubMed](#)]
24. Matta, H.; Gopalakrishnan, R.; Choi, S.; Prakash, R.; Natarajan, V.; Prins, R.; Gong, S.; Chitnis, S.D.; Kahn, M.; Han, X.; et al. Development and characterization of a novel luciferase based cytotoxicity assay. *Sci. Rep.* **2018**, *8*, 199. [[CrossRef](#)] [[PubMed](#)]
25. Schäfer, H.; Schäfer, A.; Kiderlen, A.F.; Masihi, K.N.; Burger, R. A highly sensitive cytotoxicity assay based on the release of reporter enzymes, from stably transfected cell lines. *J. Immunol. Methods* **1997**, *204*, 89–98. [[CrossRef](#)]
26. Witzel, F.; Fritsche-Guenther, R.; Lehmann, N.; Sieber, A.; Bluthgen, N. Analysis of impedance-based cellular growth assays. *Bioinformatics* **2015**, *31*, 2705–2712. [[CrossRef](#)] [[PubMed](#)]
27. Giaever, I.; Keese, C.R. A morphological biosensor for mammalian cells. *Nature* **1993**, *366*, 591–592. [[CrossRef](#)] [[PubMed](#)]
28. Langhans, B.; Ahrendt, M.; Nattermann, J.; Sauerbruch, T.; Spengler, U. Comparative study of NK cell-mediated cytotoxicity using radioactive and flow cytometric cytotoxicity assays. *J. Immunol. Methods* **2005**, *306*, 161–168. [[CrossRef](#)] [[PubMed](#)]

29. Carannante, V.; Wiklund, M.; Onfelt, B. In vitro models to study natural killer cell dynamics in the tumor microenvironment. *Front. Immunol.* **2023**, *14*, 1135148. [[CrossRef](#)]
30. Flores-Montero, J.; Kalina, T.; Corral-Mateos, A.; Sanoja-Flores, L.; Perez-Andres, M.; Martin-Ayuso, M.; Sedek, L.; Rejlova, K.; Mayado, A.; Fernandez, P.; et al. Fluorochrome choices for multi-color flow cytometry. *J. Immunol. Methods* **2019**, *475*, 112618. [[CrossRef](#)] [[PubMed](#)]

Disclaimer/Publisher's Note: The statements, opinions and data contained in all publications are solely those of the individual author(s) and contributor(s) and not of MDPI and/or the editor(s). MDPI and/or the editor(s) disclaim responsibility for any injury to people or property resulting from any ideas, methods, instructions or products referred to in the content.